

UNCLASSIFIED

AD NUMBER

AD252371

LIMITATION CHANGES

TO:

Approved for public release; distribution is unlimited.

FROM:

Distribution authorized to U.S. Gov't. agencies and their contractors;  
Administrative/Operational Use; 16 DEC 1960.  
Other requests shall be referred to Naval Ordnance Lab., White Oak, MD.

AUTHORITY

NOL ltr 29 Aug 1974

THIS PAGE IS UNCLASSIFIED

**UNCLASSIFIED**

---

**AD 252 371**

*Reproduced  
by the*

**ARMED SERVICES TECHNICAL INFORMATION AGENCY  
ARLINGTON HALL STATION  
ARLINGTON 12, VIRGINIA**



---

**UNCLASSIFIED**

NOTICE: When government or other drawings, specifications or other data are used for any purpose other than in connection with a definitely related government procurement operation, the U. S. Government thereby incurs no responsibility, nor any obligation whatsoever; and the fact that the Government may have formulated, furnished, or in any way supplied the said drawings, specifications, or other data is not to be regarded by implication or otherwise as in any manner licensing the holder or any other person or corporation, or conveying any rights or permission to manufacture, use or sell any patented invention that may in any way be related thereto.

371

CHARACTERIZATION OF SQUIB MK 1 MOD 0: 5 MEGACYCLE RF BURST SENSITIVITY

CLASSIFIED BY ASTIA  
AS AD No. 252

ASTIA  
RECEIVED  
MAR 16 1961  
TIPDR

16 DECEMBER 1960

61-2-3  
NOX



- RELEASED TO ASTIA  
BY THE NAVAL ORDNANCE LABORATORY
- ☒ Without restrictions
  - ☐ For Release to Military and Government Agencies Only.
  - ☐ Approval by BuTeps required for release to contractors.
  - ☐ Approval by BuTeps required for all subsequent release.

U. S. NAVAL ORDNANCE LABORATORY  
WHITE OAK, MARYLAND

CHARACTERIZATION OF SQUIB MK 1 MOD 0  
5 Megacycle RF Burst Sensitivity

Prepared by:  
Lawrence Green and Charles Goode

Approved by: Amos D. Solomon  
Chief, Explosion Dynamics Division

ABSTRACT: The response of the Squib Mk 1 to energy supplied as a constant current (RMS) pulse at 5 megacycles was measured. The response was compared to the results obtained with DC constant current pulses.

The results obtained were consistent with the theoretical heating:cooling model of the squib in that within experimental error the same response was obtained for both the DC and 5 megacycle cases if the RMS value of the current was used in place of the DC current value. This result is exactly as predicted by the electrothermal equations previously developed for describing the response of wire bridge electro-explosive devices.

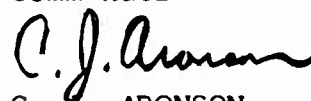
Explosions Research Department  
U. S. NAVAL ORDNANCE LABORATORY  
White Oak, Silver Spring, Md.

16 December 1960

The work reported on here has been carried out as part of the Naval Ordnance Laboratory's participation in the HERO (Hazards of Electromagnetic Radiation to Ordnance) program supported by Tasks 506-925/56015/07040, 506-925/56035/01073, and NOL-443. The objective of the HERO effort at NOL is generally to characterize the response of electro-explosive devices to electric and electro-magnetic energies. This report describes the results of tests to determine the response of the Squib Mk 1 to RF energy at a frequency of 5 megacycles.

This work should be of interest not only to the HERO project but also the broad field of electro-explosive device design, development, manufacture, and use.

W. D. COLEMAN  
Captain, USN  
Commander



C. J. ARONSON  
By direction

PUBLISHED FEBRUARY 1961

# NavWeps Report 7309

## CONTENTS

	Page
Introduction . . . . .	1
Instrumentation . . . . .	2
The RF Firing Program . . . . .	16
Conclusions . . . . .	20

## ILLUSTRATIONS

Table 1: DC Calibration of Vacuum Thermocouple . . . .	7
Table 2: C.W. Determination of Standard Impedance . .	8
Table 3: RF Burster Determination of Impedance of Reference Resistor, Pulse Width 400 Microseconds . . . . .	11
Table 4: 5 Mc RF Pulse Firing of Squib Mk 1 Mod 0 . .	22
Table 5: Energy Data Sample . . . . .	22
Figure 1: RF Burster Calibration and Firing Circuits . . . . .	3
Figure 2: DC Calibration of Vacuum Thermocouple . .	5
Figure 3: Calibration of Vacuum Thermocouple . . . .	6
Figure 4: CW Determination of Standard Impedance . .	9
Figure 5: RF Burst Firing System . . . . .	12
Figure 6: Details of Output Stage of RF Burster . .	13
Figure 7: RF Burster Auxiliary Equipment . . . . .	14
Figure 8: Firing Arrangement . . . . .	15
Figure 9: Typical RF Burster Oscillograms . . . . .	17
Figure 10: Loci of 50% Firing Points . . . . .	21

CHARACTERIZATION OF SQUIB MK 1 MOD 0 :  
5 Megacycle RF Burst Sensitivity

INTRODUCTION

One of the phases of the Squib Mk 1 Mod 0 characterization being carried out under the HERO (Hazards of Electro-Magnetic Radiation to Ordnance) program by the Naval Ordnance Laboratory is the measurement of the RF firing sensitivity of the squib. An electro-thermal model is assumed as a basis for explanation of the squib's sensitivity characteristics. (Reference (a)). A comparison between constant current DC pulse firing sensitivity and constant current RF pulse firing sensitivity would be a test of the assumed model. Such data are of direct value in the Hero program for setting RF environment tolerance levels for weapon systems. By the use of the electro-thermal model, it should be possible to predict the response of the squib to RF signals. Thus it is rather a curious fact that RF testing is being used to demonstrate that RF testing is not required in order to predict EED response to a particular RF environment.

It is possible that at much higher frequencies some initiation mechanism other than ohmic heating of the bridge-wire will "take over" to give a significantly greater EED sensitivity. Present thinking is that "exotic" initiation modes such as dielectric heating, dielectric breakdown, or bypassing of EED bridge wire would not be expected below 1,000 Mc. This thinking is in part based on the results of the work reported in Reference (b). Because unexpected initiations have occurred with the Squib Mk 1 in the communications frequencies, and because instrumentation problems seemed to be solvable by existing techniques, it was decided to begin investigation in the 5 to 10 Mc region.

- 
- Reference (a): NavOrd Report 6684, Electro-Thermal Equations for Electro-Explosive Devices, L. A. Rosenthal, 15 August 1959.
- Reference (b): NavOrd Report 6826, Characterization of the Mk 1 Mod 0 Squib, Impedance Measurements in the Frequency Range 50-1500 Megacycles, R. M. H. Wyatt, 31 May 1960.



The instrumentation that was finally used in the work discussed in the present report is described in reference (c).

# INSTRUMENTATION

Design of the RF Burster System. The burster consists of a grounded-grid, self-excited Hartley oscillator circuit, with a grounded tank coil, tunable from 4 to 9 Mc. Three 6CL6 tubes in a cathode-follower configuration, driven by a monostable-multivibrator and Schmidt trigger, in turn drive the 811 final tube from the biased to oscillating mode, and at the end of the pulse back to the biased or off condition. The multivibrator pulse width is adjustable from about 50 microseconds to about 1.4 milliseconds. The minimum usable pulse length is governed by the RF envelope pulse shape requirements. The maximum usable pulse length is governed by the duty cycle limits of the power supply and of the power tubes. The EED is connected in series with a reference resistor and a power-pick-off coil. The coil is inductively coupled to the tank circuit, being mounted concentrically with it on a longitudinally movable trolley. The pulse amplitude applied to the EED is controlled by varying the coupling between tank and pick-off coils brought about by positioning the trolley. The trolley not only supports the pick-off coil, reference resistor, and EED, but it also protects the burster circuitry from blast, fragments, and combustion residue from the exploding EEDs. The EED and the reference resistor are arranged in a balanced relationship as shown in Figure 1(a). (In order to obtain isolation between the two sides it was necessary to install a grounded electrostatic shield, which can be seen in Figure 6.)

Calibration of the RF Burster. The reference resistor is employed to monitor and measure the current envelope of the RF burst. The EED will change resistance (and therefore impedance) as it heats up. By CRO monitoring of the waveform across both the EED and the reference resistor it is possible to measure not only the EED pulse width and amplitude but also the pulse energy content. Two assumptions are inherent in this design:

-----  
Reference (c): NavWeps Report 7354: A Radio Frequency  
Burst Source for Electro-Explosive Device  
Testing, L. A. Rosenthal (not yet published).

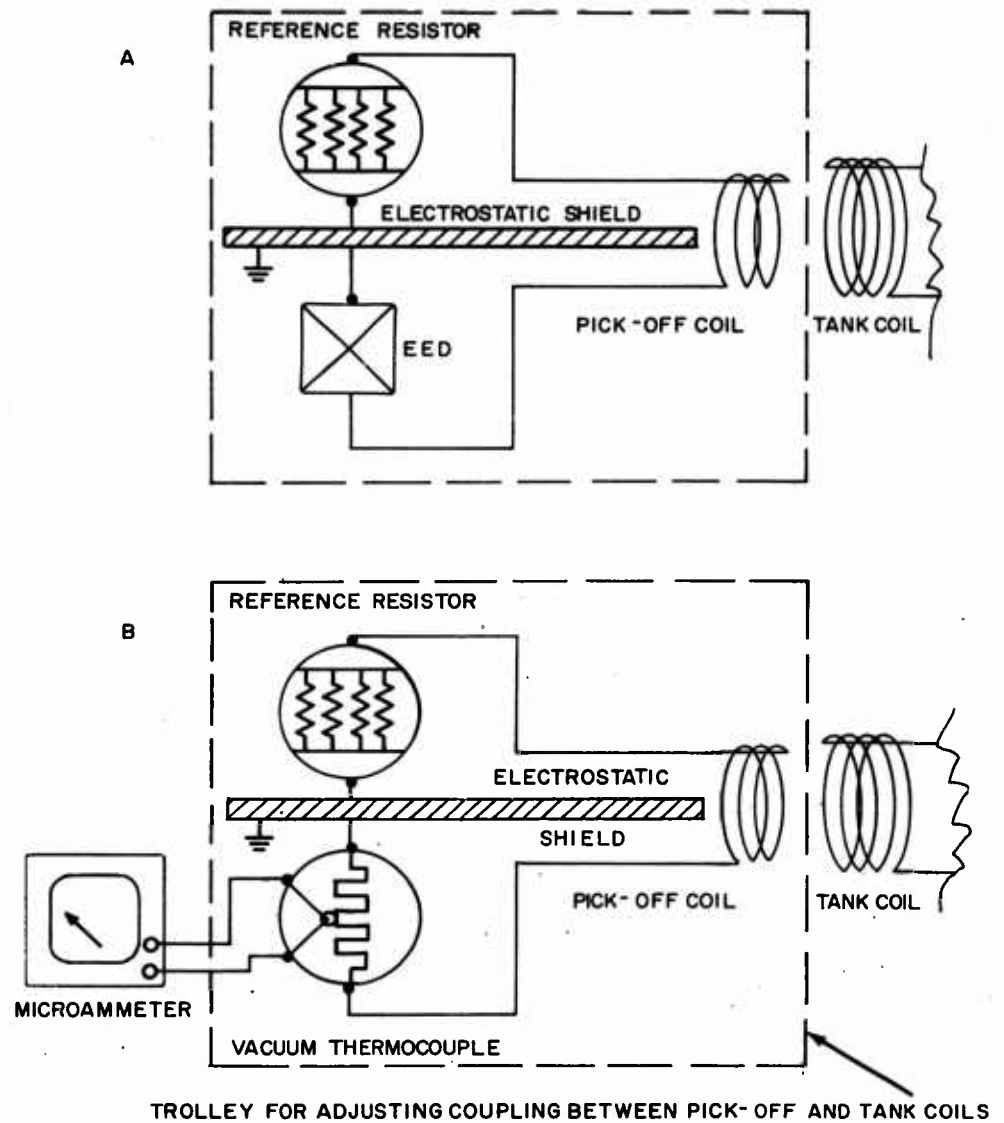


FIG.1 RF BURSTER CALIBRATION AND FIRING CIRCUITS

- (a) The currents through the EED, the reference resistor, and pick-off coil are all the same. That is, there is no capacitive shunting or bypassing of any of the three components.
- (b) The impedance of the coil is so high that changes in the EED impedance will not change the current amplitude.

The reference resistor was constructed by paralleling eight 10-ohm resistors in a low-inductance, low-capacitance arrangement. This resistance, for maximum utility, should be of the same order of magnitude as the EED impedances.

The accuracy of the measurement of the pulse amplitude depends on the accuracy of the determination of the reference resistor impedance. The obvious technique for measuring impedance by use of the Q-meter does not yield satisfactory results because of the very low impedances involved.

As a result of the difficulty with the Q-meter, it was decided to determine the impedance of the reference resistor by the "volt-ammeter" method, using a carefully calibrated Number 10, insulated heater, vacuum thermocouple to read the RMS-RF current. The simultaneous determination of the potential across the reference resistor permits the computation of the resistor's impedance. The potential drop can be measured readily by cathode ray oscillography.

In order to know the relationship between the vacuum thermocouple output signal and the RMS-RF current (assuming true sinusoidal RF wave form) it is necessary to determine the DC-equivalent sensitivity. That is, it is necessary to find the thermocouple output potential as a function of input heater current. Using the experimental setup shown in Figure 2, the data given in Table I were obtained. The data of Table I are plotted in Figure 3. As can be seen in Figure 2, two instruments were used to read the thermocouple output; the Hewlett-Packard Model 425AR microvolt ammeter to read the output at low levels, and the John Fluke Type 801 differential voltmeter at the high levels.

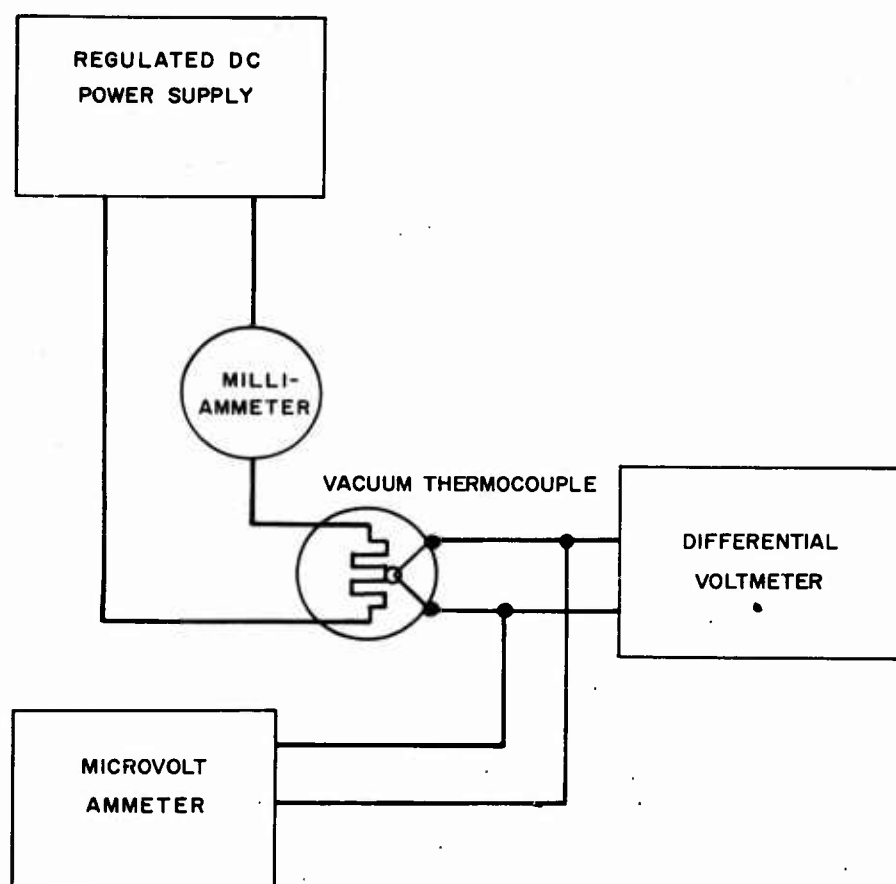


FIG.2 DC CALIBRATION OF VACUUM THERMOCOUPLE

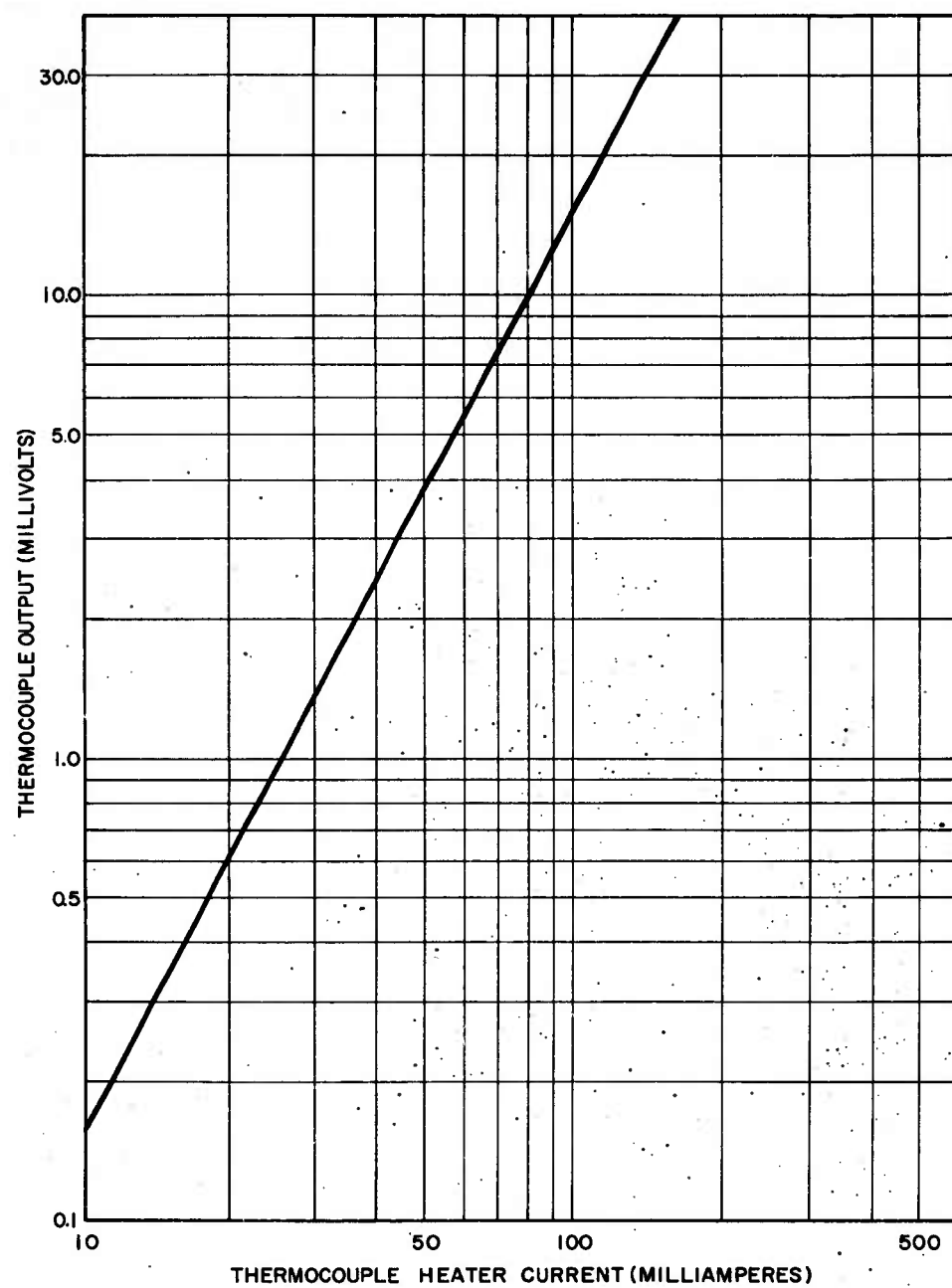


FIG.3 CALIBRATION OF VACUUM THERMOCOUPLE

Table 1  
DC Calibration of Vacuum Thermocouple No. 1

Heater Input Current (milliamperes)	Thermoelectric Potential Output (millivolts)	$K = V_{VT}/I_{eff}^2$
40	2.50	1.56
50	3.9	1.56
60	5.7	1.58
70	7.7	1.57
80	10.1	1.58
90	12.8	1.58
100	15.7	1.57

The temperature rise of the thermocouple heater is described by the general heat balance equation:

$$C_p \frac{d\theta}{dt} + \gamma \theta = I^2 Z_{VT} \cos \phi = I^2 R_{VT}$$

or in steady state:

$$\theta_f = \frac{I^2 R_{VT}}{\gamma} = C_1 I^2$$

where  $C_p$  is the heat capacity of the heater

$\theta$  is the temperature rise above ambient

$\gamma$  is the heat loss factor

$I$  is the heater current

$Z_{VT}$  is the impedance

$R_{VT}$  is the DC resistance, and

$\phi$  is the phase angle.

The steady state equation holds as long as the DC resistive component undergoes no change. The emf generated by the thermojunction is:

$$V_{VT} = C_2 (\theta_2 - \theta_1), \text{ and if}$$

$\theta_1$ , the cold junction temperature, is at ambient

$$V_{VT} = C_2 \theta_f = C_1 C_2 I_{eff}^2 = K I_{eff}^2$$

(Here  $C_1$  and  $C_2$  are constants which combine to give the constant  $K$ .)

The constant, K, therefore relates the observed output of the thermojunction to the heater current input. The values of K for thermocouple No. 1 are shown in Table 1, the average value used in subsequent calculations being 1.57. The value for thermocouple No. 2 was 1.12. \*

Since the value of K is sensitive to heater resistance variations, a heater volt-ampere characteristic was determined. The results showed that the resistance was constant throughout the range of heater currents used.

To verify the value of K as determined by the DC method, a number of checks were made using RF power. The vacuum thermocouple and a Weston Model 622 RF milliammeter were driven in series by the RF burster. The scale of the RF milliammeter covered only a small portion of the desired range. The two indicators agreed well within the reading error of the RF milliammeter. Another check was made by driving the vacuum thermocouple and the reference resistor in series with a General Radio Type 1211B unit oscillator as shown in Figure 4, with the results as shown in Table 2.

Table 2

## C.W. Determination of Standard Impedance

$V_{VT}$ (millivolts)	$I_{eff}$ (milliamperes)	$V_{pp}$ (volts)	$Z$ (ohms)
2.2	37.4	0.153	1.44
4.63	54.3	0.221	1.44
7.81	70.5	0.285	1.43
9.62	78.3	0.316	1.43
11.72	86.4	0.345	1.41
13.53	92.8	0.369	1.41
15.13	98.2	0.390	1.41

To check for the possibility of an asymmetrical current flow on the two sides of the electrostatic shield, measurements were made with the arrangement as shown in Figure 1(b). The reference resistor and the vacuum thermocouple were then interchanged and the measurements were repeated. Within the reading error of the system, the potential drop across the vacuum thermocouple and across the reference resistor were found to be independent of their locations.

\* Two thermocouples were checked in the experiment to observe the variability from one to another.

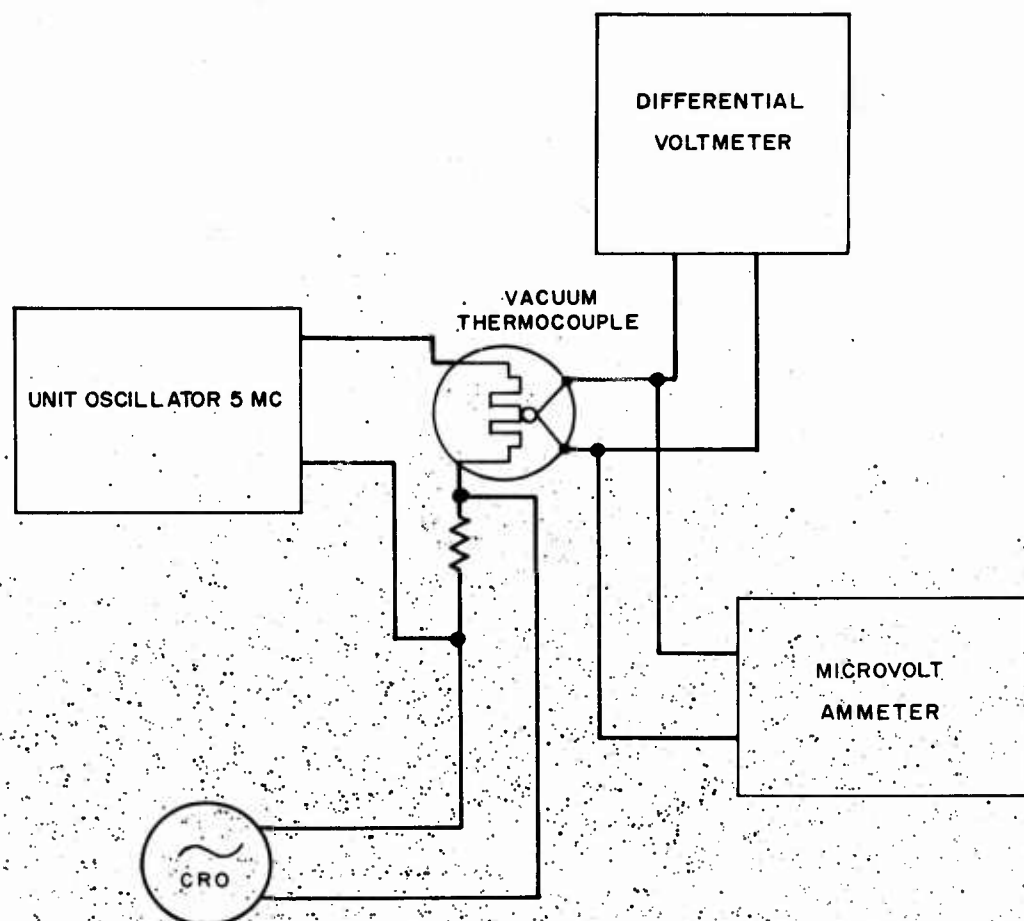


FIG. 4 CW DETERMINATION OF STANDARD IMPEDANCE



The impedance of the reference resistor,  $Z_R$ , can be measured by the arrangement shown in Figure 1(b), once the vacuum thermocouple has been calibrated. When the RF burster is operated in the repetitive mode, the effective pulse amplitude can be computed on the basis of the duty cycle,  $D$ , and the peak-to-peak pulse amplitude observed across the reference resistor.

$$V_{\text{eff}} = \frac{V_{\text{pp}}}{2\sqrt{2}} \sqrt{D}$$

$$= \frac{V_{\text{pp}}}{2\sqrt{2}} \sqrt{W \cdot \text{PRF}}$$

where  $V_{\text{eff}}$  is the RMS drop across the reference resistor,

$V_{\text{pp}}$  is the observed peak-to-peak drop across the reference resistor,

$W$  is the pulse width, and

PRF is the pulse repetition frequency.

The effective current,  $I_{\text{eff}}$ , can be found from the vacuum thermocouple indication,  $V_{\text{VT}}$ ,

$$I_{\text{eff}} = \sqrt{\frac{V_{\text{VT}}}{K}}$$

The impedance of the reference resistor will therefore be given by:

$$Z_R = \frac{V_{\text{eff}}}{I_{\text{eff}}}$$

$$= \frac{V_{\text{pp}}}{2\sqrt{2}} \sqrt{\frac{K \cdot W \cdot \text{PRF}}{V_{\text{VT}}}}$$

Using thermocouple No. 1 this can be evaluated as

$$Z_R = 3.431 V_{\text{pp}} \sqrt{\frac{W}{V_{\text{VT}}}}$$

for a PRF of 60 cycles per second.

Measurements made by this technique yielded the results listed in Table 3. It can be seen that these results are in excellent agreement with those obtained by the CW method, Table 2.

Table 3

RF Burster Determination of Impedance  
of Reference Resistor  
Pulse Width 400 Microseconds

$V_{VT}$ (millivolts)	$V_{PP}$ (volts)	$Z_R$ (ohms)
4.71	1.42	1.42
6.33	1.65	1.42
8.21	1.87	1.42
11.20	2.19	1.43
12.53	2.31	1.42
14.22	2.47	1.42
16.25	2.62	1.41

Experimental Firing Setup. Details of the equipment are shown in Figures 5, 6, 7, and 8. Figure 5 is a photograph of the firing system showing the two Model 545 Tektronix CROs with oscillograph cameras, and the burster. Two separate cameras were used, one to record the signal across the reference resistor, and the other the signal across the EED. While it is possible to display both signals on a single CRO by the use of a dual beam preamplifier, it was found that the two CRO method permitted the use of the full screen for each record, thereby giving greater definition. Details of the pick-off coil, tank coil, pick-off coil trolley, and electrostatic shield can be seen in Figure 6. The low current ohmmeter (used to measure the EED cold resistance) and details of the Fiberglas EED safety chamber are shown in Figure 7. The chamber was used to handle the EEDs both during non-destructive tests and during firing operations. They were designed to give operator protection in case of inadvertent firing. During intentional firing the safety chambers were further confined in the trolley previously mentioned as an additional precaution. Figure 8 is a schematic diagram of the firing system.

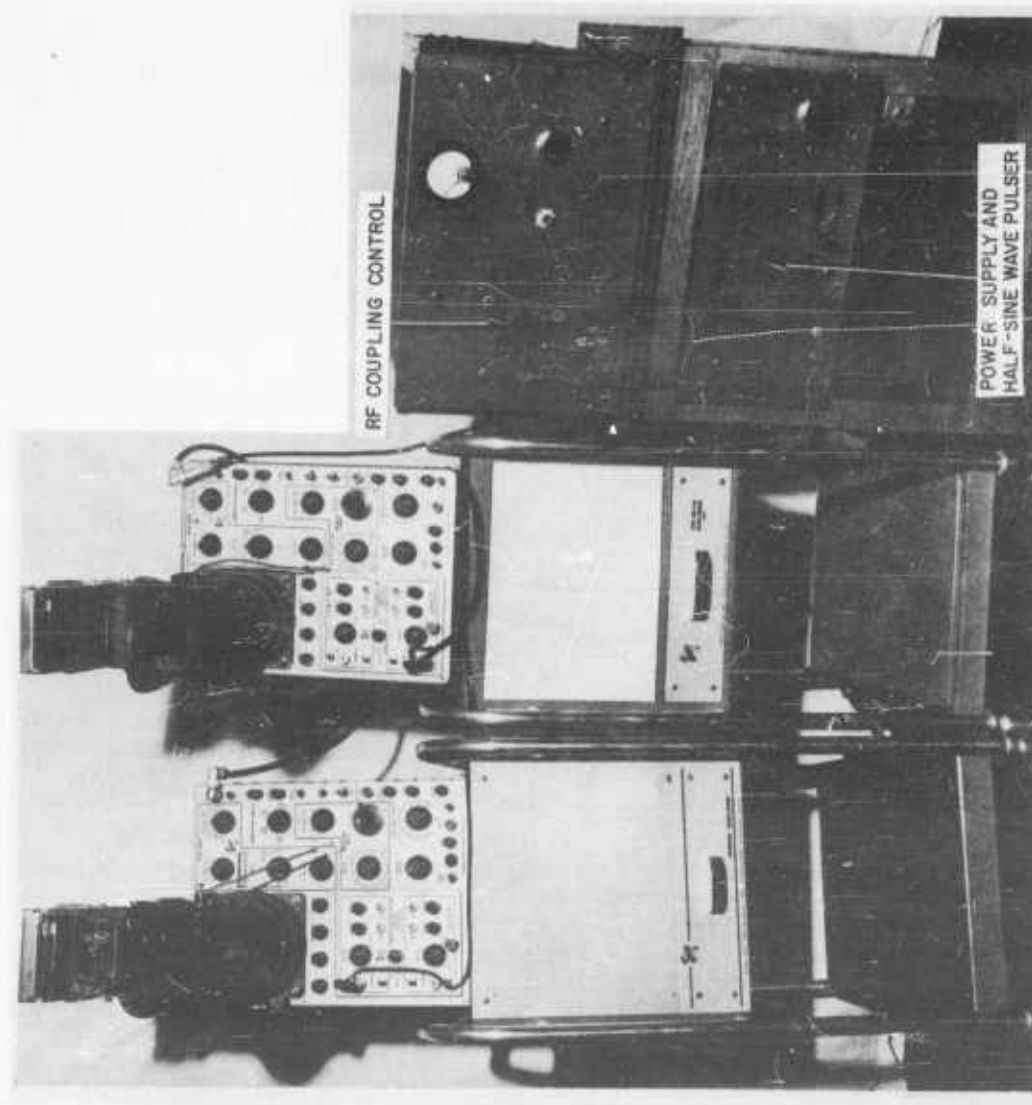


FIG. 5 RF BURST FIRING SYSTEM

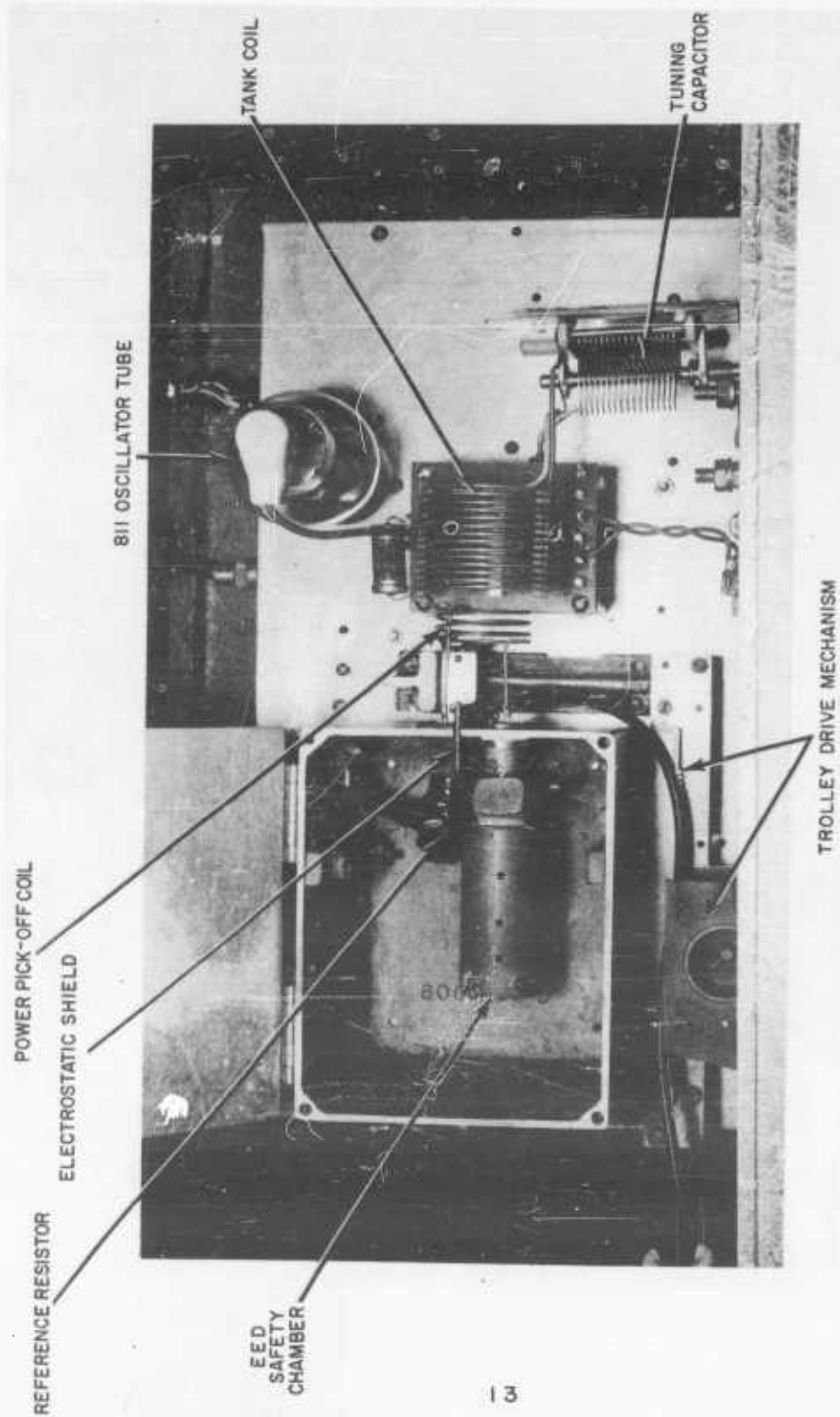


FIG.6 DETAILS OF OUTPUT STAGE OF RF BURSTER

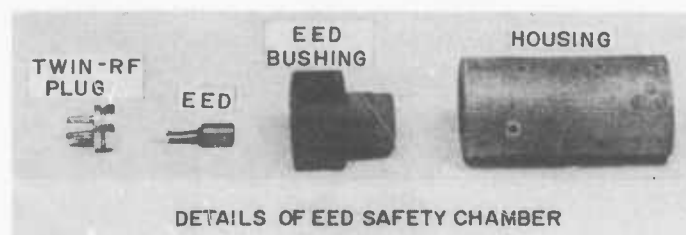
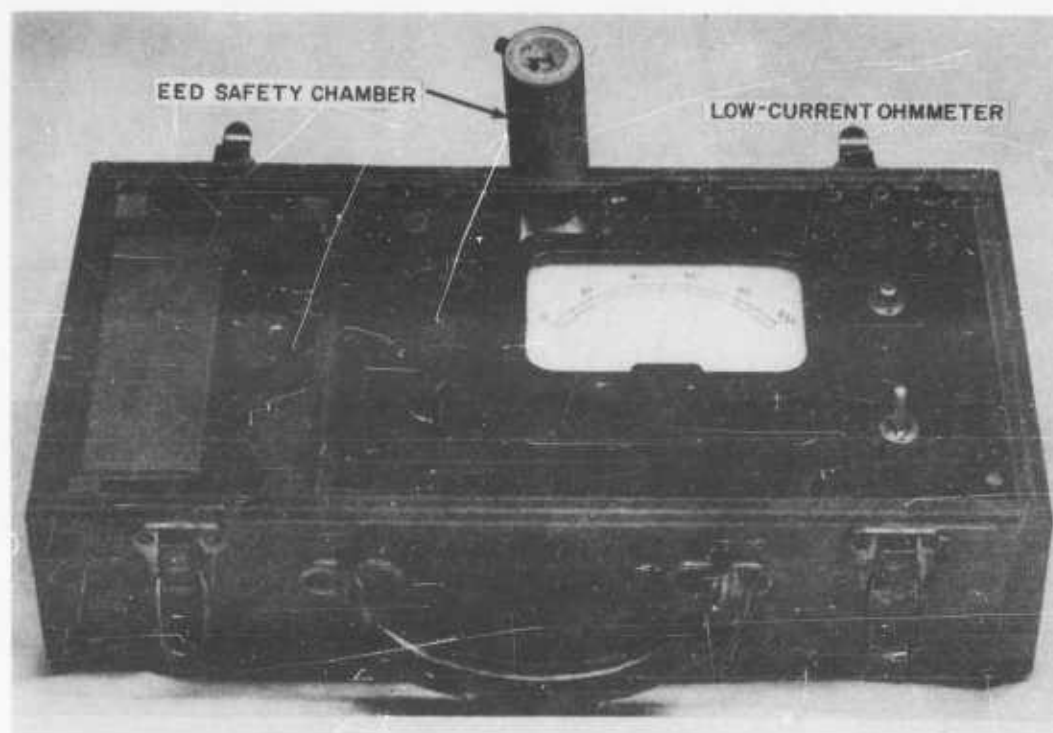


FIG.7 RF BURSTER AUXILIARY EQUIPMENT

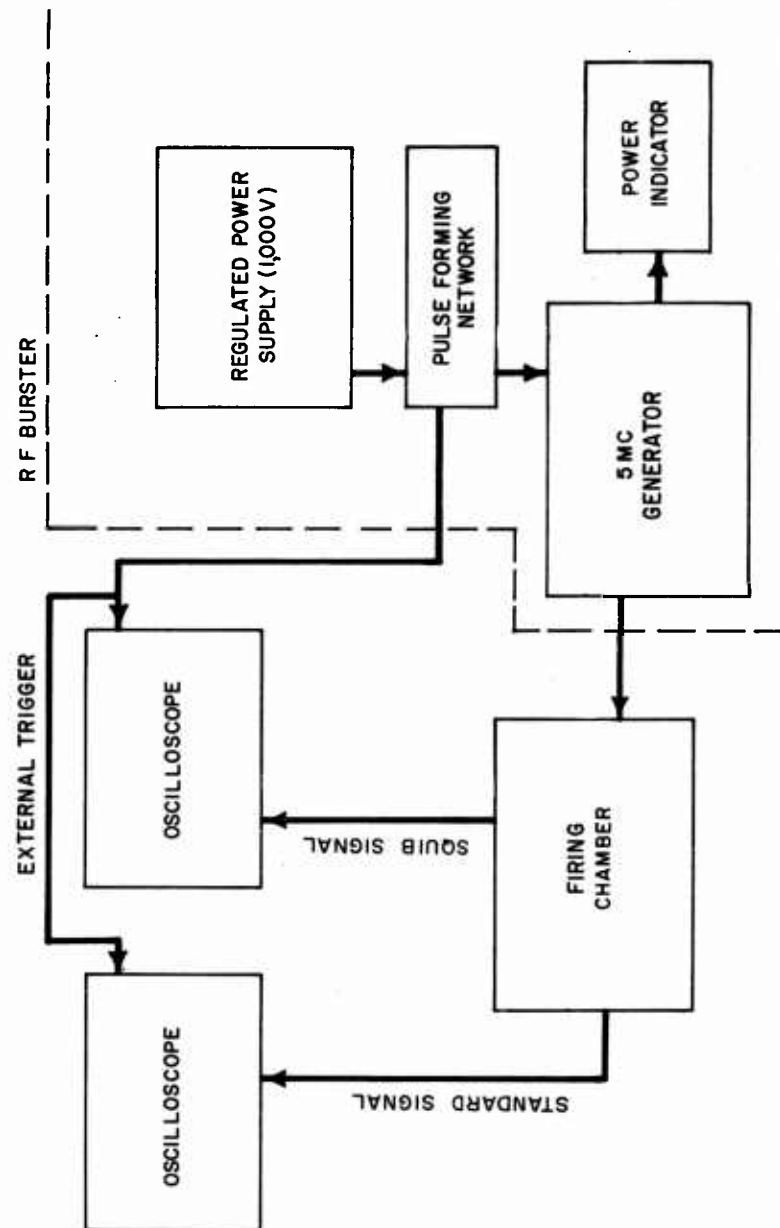


FIG. 8 FIRING ARRANGEMENT

## THE RF FIRING PROGRAM

Design of Experiment. In order to compare RF firing data directly with the results of the DC constant current burst firings, the peak-to-peak current through the squib must be set at some predetermined value and the pulse width varied according to a Bruceton test plan to obtain the 50% firing time at that current value. Both time and current settings are made by replacing the squib with a resistor of approximately the same impedance. The pulse height need, of course, be changed only once for each series of firings; the pulse width after each firing in the run.

The Form of the Data. Figures 9(a), 9(b), and 9(c) are photographs of the standard trace at the pulse widths and current values indicated. In all cases the pulse envelope indicates constant current for the duration of the firing (except for a short rise time). The peak-to-peak voltage is read using a Telecomputer Telereader, and the peak current is obtained by dividing this by the standard impedance, 1.42 ohms.

Figures 9(d), 9(e), and 9(f) are squib trace photographs. An increase in the impedance of the squib with time may be easily seen. It is interesting to note that this change, caused by an increase in the DC resistance of the bridge wire as a result of its ohmic heating, is reflected into the impedance change as a linear variation.

Treatment of Data (Theory). An infinitesimal change in the bridge wire temperature is given by

$$d\theta = dQ/C_p$$

$$= \frac{I_{\text{eff}}^2 R(t)}{J C_p} \cdot dt$$

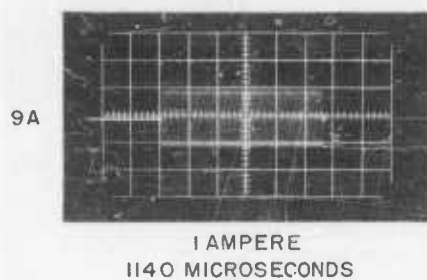
where  $C_p$  is the heat capacity of the wire in calories/degree,

$I_{\text{eff}}$  is the constant effective current delivered during the RF burst,

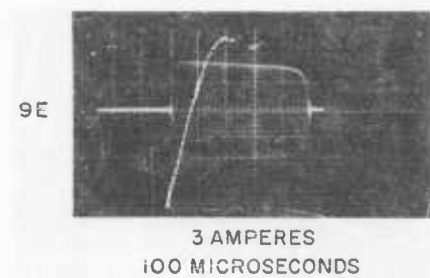
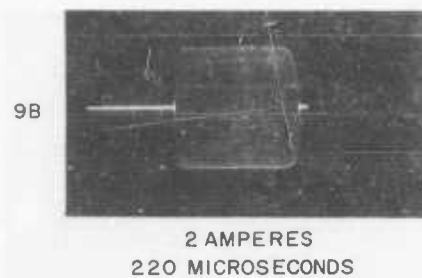
$J$  is the joule equivalent in joules/calorie, and

$R(t)$  is the time dependent value of resistance.

REFERENCE RESISTOR WAVEFORMS



EED WAVEFORMS



TIME INCREASES  
RIGHT TO LEFT

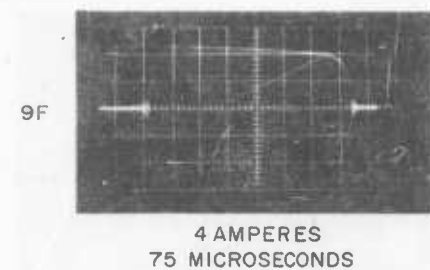
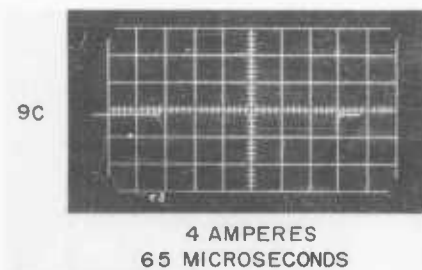


FIG.9 TYPICAL RF BURSTER OSCILLOGRAMS



The resistance change is known to be linear and is therefore given by:

$$R(t) = R_0 (1 + \alpha \theta)$$

where  $\theta$  is the temperature rise above ambient

$R_0$  is the ambient resistance, and

Then:

$\alpha$  is the thermal coefficient of resistivity.

$$d\theta = \frac{I_{\text{eff}}^2 R_0}{J C_p} (1 + \alpha \theta) dt$$

and

$$\int_0^\theta \frac{d\theta}{1 + \alpha \theta} = \frac{I_{\text{eff}}^2 R_0}{J C_p} \int_0^t dt.$$

Integrating and rearranging terms the temperature variation is:

$$\theta = \frac{1}{\alpha} [\exp(kt) - 1]$$

where

$$k = \frac{I_{\text{eff}}^2 R_0 \alpha}{J C_p}.$$

Substitution into the equation giving  $R$  as a function of  $\theta$  yields

$$R(t) = R_0 \exp(kt).$$

The only assumption made thus far is that the energy is applied to the bridge wire ballistically. Since the bridge wire time constant is of the order of several milliseconds, the assumption is valid at the higher current levels but is not applicable at the longer pulse width-low amplitude levels.

The time variation of the squib voltage is given by

$$V_{\text{eff}}(t) = I_{\text{eff}} \sqrt{X^2 + R(t)^2} =$$

$$I_{\text{eff}} \sqrt{X^2 + R_0^2 \exp(2kt)}$$

Q-meter measurements have indicated a reactance on the order of 0.3 ohm. The first term under the radical is therefore negligible in comparison with the second. Since  $kt$  is a small quantity also, we may expand the exponential:

$$V_{\text{eff}}(t) = I_{\text{eff}} R_0 [1 + kt].$$

The energy delivered in time  $(t)$  is therefore

$$E = I_{\text{eff}}^2 R_0 [t + kt^2].$$

These equations were derived to illustrate consistency of the experimental results, but will not be used here in actual computation. The energy delivered to the squib during each firing may be obtained directly from the film record, without the necessity of knowing  $k$ . In fact, the slope of the squib voltage trace ( $I_{\text{eff}} R_0 k$ ), may be used to obtain  $k$  for each bridge wire tested.

Since the resistance variation is nearly linear with time the energy delivered is also given approximately by

$$E = I_{\text{eff}}^2 \bar{R} t \quad \text{with} \quad \bar{R} = \frac{R_0 + R_f}{2}$$

where  $R_f$  is the resistance at the end of time  $t$ . The time  $t$  is merely the pre-set pulse width, and the final resistance  $R_f$  may be determined as follows:

The initial impedance is

$$Z_i^2 = R_0^2 + X^2.$$

The final impedance is similarly given by

$$Z_f^2 = R_f^2 + X^2$$

where the reactance has remained unchanged.

Subtracting the first equation from the second and solving for  $R_f$  we have

$$R_f = \sqrt{Z_f^2 - Z_i^2 + R_0^2}.$$

The cold resistance  $R_0$  of each squib is measured before firing.  $Z_i$  and  $Z_f$  are determined from the photos by measuring the initial and final voltage drop and dividing by the corresponding current.

Results. Figure 10 and Table 4 summarize the results of the experiment as far as comparison with the DC burst data is concerned. Four different current values were investigated, and the 50% points obtained for each of these points by a 40-shot Bruceton run. It may be seen that, within experimental error, these points fall along the loci of 50% points obtained in the DC firing. The observations at two amperes appear to be unexpectedly variable, the standard deviation being 5 to 10%. This was the first run on the Burster and measurement and test techniques had not been fully developed. The Bruceton run appeared to be made up of two statistically incompatible segments; one yielding a mean of 210 microseconds and a standard deviation of 11 microseconds, and the other a mean of 156 and a standard deviation of 18. Since there is no basis for rejecting either half, the two segments are combined.

Table 5 illustrates the data taken in the energy determinations. The values of  $Z$  listed appear too high since there is some coupling between the leads running from the squib to the oscilloscope and the tank circuit. This does not, of course, affect the final energy determination. These energies are approximately the same as those obtained on the DC basis.

#### CONCLUSIONS

At 5 Mc it is concluded that the initiation sensitivity of the Squib Mk 1 Mod 0 is as would be predicted on the basis of the electro-thermal model assuming that the explosive is initiated only by the thermal transfer from the EED bridge wire which, in turn, is brought to an elevated temperature only by the "ohmic heating" due to the power of the RF burst. At the 2-ampere level, the unusually large standard deviations, both in the observed energy and observed pulse widths, are not thought to be a property of the EED but rather were probably due to techniques which were later refined with experience.

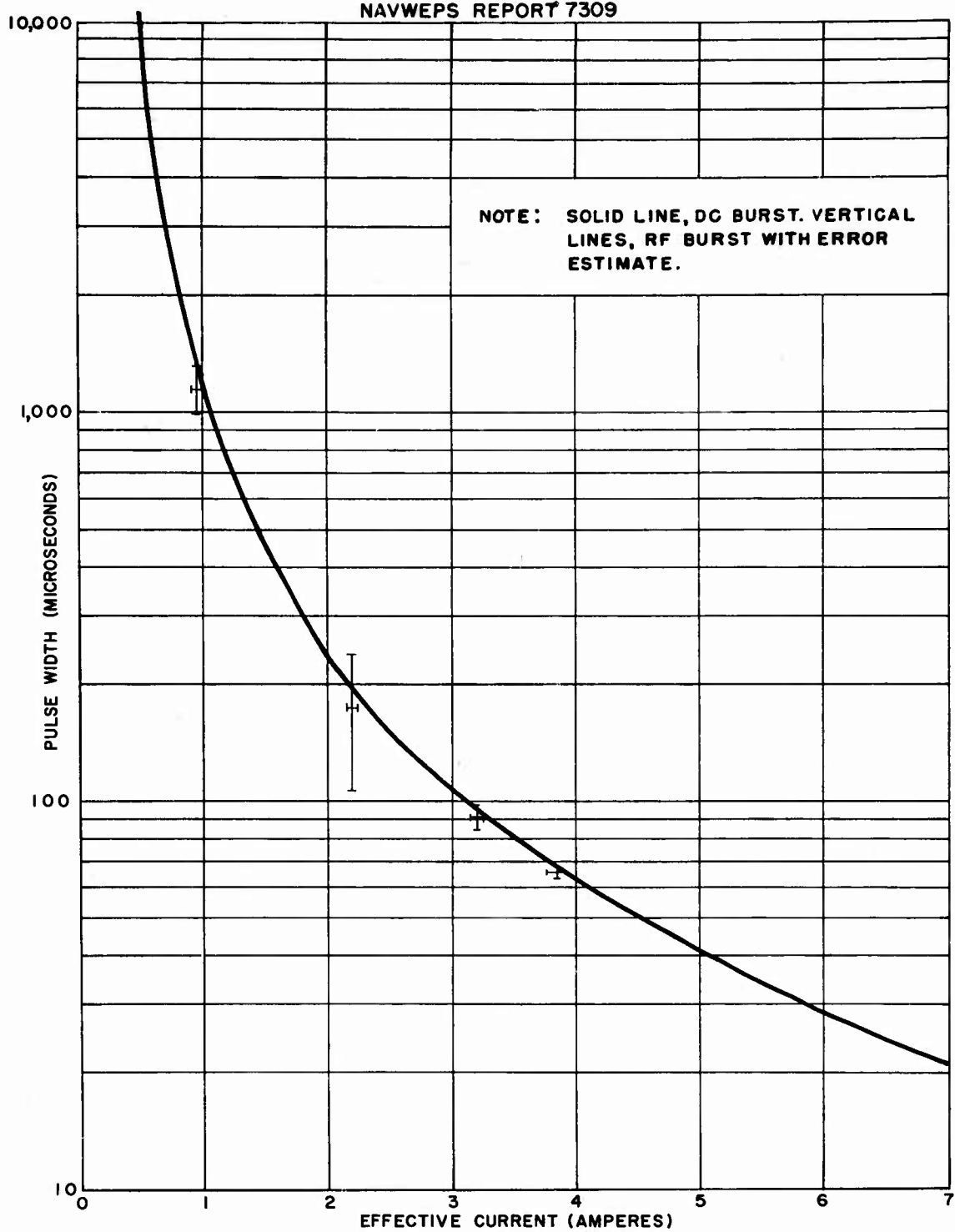


FIG.10 LOCI OF 50% FIRING POINTS

Table 4

## 5 Mc RF Pulse Firing of Squib Mk 1 Mod 0

<u>Pulse Amplitude</u> <u>(Amperes RMS)</u>		<u>Pulse Width</u> <u>(Microseconds)</u>		<u>Pulse Energy Content</u> <u>(Millijoules)</u>	
<u>I</u>	<u>s</u>	<u>T</u>	<u>s</u>	<u>E</u>	<u>s</u>
0.962	0.036	1,154	168	-	-
2.19	0.037	173	66	1.135	0.225
3.19	0.039	91.1	6.9	-	-
3.84	0.056	65.9	2.8	-	-

Table 5

## Energy Data Sample

<u>Squib</u> <u>No.</u>	<u>Pulse</u> <u>Time</u> <u>(micro-</u> <u>sec.)</u>	<u>Z<sub>i</sub></u> <u>(ohms)</u>	<u>Z<sub>f</sub></u> <u>(ohms)</u>	<u>R<sub>i</sub></u> <u>(ohms)</u>	<u>R<sub>f</sub></u> <u>(ohms)</u>	<u>R̄</u> <u>(ohms)</u>	<u>Energy</u> <u>(millijoules)</u>
1	160	1.71	1.97	0.953	1.37	1.16	0.94
2	180	2.03	2.34	1.16	1.64	1.40	1.19
3	200	1.81	2.10	0.859	1.37	1.11	1.13
4	180	1.77	2.10	0.965	1.49	1.23	1.08
5	160	1.81	2.07	0.992	1.41	1.18	0.89
6	140	1.71	1.96	0.965	1.36	1.16	0.75
7	160	1.83	2.16	1.02	1.53	1.27	0.91
8	140	1.57	1.87	0.996	1.30	1.14	0.74
9	160	1.73	2.02	0.992	1.44	1.22	0.90
10	180	1.73	2.06	0.898	1.43	1.16	1.03

All readings taken at 2-ampere current level.